

# Effects of the anomalous magnetic moments of the quarks on the neutral pion properties within a SU(2) Nambu-Jona Lasinio model

R. M. Aguirre\*

Facultad de Ciencias Exactas, Universidad Nacional de La Plata and Instituto de Fisica La Plata, Argentina

## Abstract

The properties of the neutral pion in quark matter under the influence of an external magnetic field are studied. The effects of the anomalous magnetic moments (AMM) of the quarks at finite density is considered. The inclusion of the AMM into the NJL model gives rise to additional magnetic effects. In particular the Dirac sea produce new divergences in the vacuum contributions, which depend explicitly on the magnetic field. An improper treatment of these contributions is the source of unphysical results, as emphasized in recent investigations. The pion polarization function is evaluated in the random phase approximation using analytic regularization and a subtraction scheme to deal with such divergencies. This procedure is combined with the standard three momentum cutoff, and reduces to it for vanishing magnetic intensity. The pion mass and coupling constant are evaluated for a wide range of magnetic intensity and baryonic density.

## 1 Introduction

The study of the strong interaction under the influence of different external agents will eventually shed light on the complexity of its phase diagram, or could reveal new unknown features. In particular the analysis of the low energy regime resorts to specific tools such as lattice simulation and effective models, due to the intricacies of the fundamental theory. Within the last mentioned case, the Nambu-Jona Lasinio (NJL) model has shown to be a useful conceptual recourse to tackle different problems. It has been extensively used to include the effects of finite temperature, matter density, isospin composition and electromagnetic fields in strong interacting systems [1, 2, 3, 4]. As a special chapter of this approach one can mention the study of quarks interacting with external magnetic fields [5, 6, 7, 8, 9, 10, 11, 12, 13, 14, 15], where a variety of issues have been analyzed such as magnetic catalysis [7], magnetic oscillations [8], color superconductivity [9, 10, 12, 15], chiral density waves [11], vector [13] and tensor [14] additional couplings. The relation to experimental observables has also been considered, as for instance the dilepton rate production [16] and the scattering cross section of charged mesons [17].

Theoretical treatments based on the local field theory are compelled to give a proper definition of the vacuum contributions under the presence of an external magnetic field [18, 19, 20, 21, 22]. Ref. [18] provides general expressions for the effective action of a Dirac field interacting with a magnetic field for intensities  $B$  greater than the mass scale. A description based on the chiral sigma Lagrangian has been made in [19], [20] uses the quark-meson model, whereas in [21] the vacuum contribution to the magnetization is evaluated in a one-loop

---

\*e-mail: aguirre@fisica.unlp.edu.ar

approach to QCD for very intense magnetic fields. Using the chiral quark model and a Ginzburg-Landau expansion Ref. [22] has found that different treatments of the divergences could yield important modifications of the phase diagram.

This discussion is particularly significant for the NJL model since its main feature is the breakdown of the Lagrangian chiral symmetry through the vacuum condensates. Therefore the magnetic effect on the model has been widely debated [2, 7, 8, 23, 24, 25, 26, 27, 28, 29, 30, 31, 32]. The evaluation of the effective potential following the analytic regularization in terms of the Hurwitz zeta function in Ref. [8] leads to a divergence depending on the squared magnetic intensity. To dispose of this singularity, the authors propose a wavefunction renormalization by associating it to the pure magnetic contribution to the energy density. The same divergent term has been recently exhibited in the evaluation of the thermodynamic potential [25]. Furthermore, in a recent paper [33] this author have shown that the inclusion of quark anomalous magnetic moments in a SU(2) NJL model introduce additional divergences depending on  $B^2$ .

The use of different regularization procedures should not lead to qualitative discrepancies in the physical observables. However, it has been found [29, 30] that the use of smooth form factors instead of a steep cutoff could change drastically the physical predictions. Particularly Ref. [30] points out that the key point is to clearly distinguish between the non-magnetic vacuum contribution from the magnetic one. A failure in this point should be the cause of the inadequate behavior found in different calculations, such as tachyonic poles in the spectrum of light mesons and unphysical oscillations in thermodynamical quantities.

Among the diverse procedures used to deal with the divergences one can find softening regulators, as used in [31] or sharp step functions [32]. In both cases there is an explicit mixing of the integration momentum variable and the magnetic intensity. More sophisticated is the treatment given in [34], where analytical regularization is used to separate singularities as poles of the gamma function. Then the integral representation of the gamma is used modifying its range of integration to avoid divergences. A method to write the thermodynamical potential as the sum of terms, one of which isolate the divergence and does not depend on B, was presented in [24]. The authors proposed that this can be achieved by subtracting and adding the pressure  $P_0$  at zero baryonic density and finite  $B$ . In the former case  $P_0$  still have the undesirable divergence and in the latter one it has been regularized in the 3-momentum cutoff scheme.

An interesting aspect of the dynamics of quarks in a magnetic field is the discrepancy of their gyromagnetic factors from the ideal value 2. This issue have been considered for a long time [35, 36, 37] and has received renewed interest recently [14, 31, 32, 33, 38, 39, 40]. From a phenomenological point of view one can take as a reference for the magnetic moments of the light quarks the prediction of the non relativistic constituent quark model. In order to adjust the experimental values of the proton and neutron magnetic moments, the gyromagnetic ratios  $\tilde{g}_u = 2\mu_u/\mu_N = 3.7$ ,  $\tilde{g}_d = 2\mu_d/\mu_N = -1.94$  are obtained within this approach. Given the constituent mass  $M$  and the electric charge  $Q_f = q_f e$  of a quark of flavor  $f$ , its AMM can be estimated as  $a_f = (2\tilde{g}_f M/q_f M_p) - 1$ , where  $e$  and  $M_p$  are the proton charge and mass respectively.

The AMM of the quarks arises in close relation to the breakdown of the chiral symmetry. For this reason the NJL model with zero current quark mass have been used to study the origin of the AMM [14, 35, 36]. To analyze the feasibility of the dynamical generation of the AMM, in [35] a one loop correction to the electromagnetic vertex is evaluated within the one flavor NJL model, obtaining

$$\tilde{g} \approx \frac{2M_p}{M} \frac{e_q}{e} [1 - (M/\Lambda)^2 \log(\Lambda/M)].$$

In the approach of [36] the AMM is extracted from the low momentum electromagnetic current written in terms of the kernel of the Ward identities. Assuming a four momentum cutoff, they find zero AMM in a one flavor NJL model. However, by using the two flavor version, the authors obtain  $\tilde{g}_u \approx 3.813$ ,  $\tilde{g}_d \approx -1.929$ , which differ from the phenomenological expectations by less than 1%. Furthermore, in the same work an schematic

confining potential for only one flavor is considered. By taking a constituent quark mass  $M = 330$  MeV, typical of the NJL model, the magnitude of the predicted AMM is as large as 0.15.

Another point of view is developed in [14], where the one flavor NJL model is supplemented with a four fermion tensor interaction, which induces a condensate in the  $\gamma^1 \gamma^2$  channel. In this case the intrinsic relation between the constituent quark mass and its AMM is explicitly exposed, since the vacuum condensate which breaks the chiral symmetry is also responsible for the occurrence of nonzero AMM. As a consequence, the AMM has a non-perturbative dependence on the magnetic intensity.

The necessity of the AMM of the quarks has been emphasized in [37] in the context of the Karl-Sehgal formula, which relates baryonic properties with the spin configuration of the quarks composing them. By stating the dynamical independency of the axial and tensorial quark contributions to the baryonic intrinsic magnetism, the AMM of the quarks are proposed as the parameters that distinguish between them. Resorting to sound arguments, the author propose  $a_u = a_d \approx 0.38$ ,  $a_s \approx 0.2 - 0.38$  as significative values for the AMM for the lightest flavors.

Other investigations have focused on the consequences of a linear coupling between a phenomenological AMM and an external magnetic field [31, 32, 41]. For instance, [31] analyze the phase diagram of the NJL at finite temperature, with special emphasis on a possible chiral restoration due to the non-zero AMM. Furthermore, the possibility of a non linear coupling of the AMM of the quarks is also considered. In this model the AMM is related to the quantum correction to the electrodynamic vertex, and a non-perturbative dependence on the magnetic field is introduced through the effective constituent quark mass. The influence of the AMM on the structure of the lightest scalar mesons is analyzed in [32], while [41] is devoted to study their effects on neutral and beta stable quark matter within a bag model.

The aim of the present work is to study how some properties of the neutral pion are modified in the presence of a magnetic field due the changes in its internal structure.

Similar studies, focusing on different light mesons within several effective models, have been performed in the last years. For instance, kaons [42] and pions [43] were studied in effective hadronic models, pions in the linear sigma model [44, 45], and also in the NJL model [28, 29, 32, 46, 47].

Effective quarks are considered in the present work, with medium dependent masses and nonzero AMM. The calculations are performed by using a quark propagator which includes the anomalous magnetic moments and the full interaction with the external magnetic field [33]. As already mentioned, there is recently published material covering the same subject [31, 32]. However, the main difference with such works is the treatment of the vacuum contributions. In the cited references the ultraviolet divergences are avoided by restricting the range of the integrals in a way that depends on the magnetic intensity. In the case of [31] the cutoff parameter  $\Lambda$  is inspired by a covariant 4-momentum scheme  $E_{n_s}(p, B) < \Lambda$ , where  $E_{n_s}(p, B)$  represents the energy of the  $n$ -th Landau level with spin projection  $s$  along the direction of the uniform magnetic field. Ref. [32], instead, uses a 3-momentum cutoff  $p < \sqrt{\Lambda^2 + M^2 - E_{n_s}(0, B)^2}$ . In contrast, a complete analytical regularization is given here, that clearly separates finite magnetic dependency. Since the regularization procedure for  $B = 0$  is an intrinsic part of the NJL model, the results obtained reduce to the standard vacuum expressions for vanishing magnetic field.

This work is organized as follows. In the next section a summary of the NJL model complemented with a linear coupling for the AMM is presented and the regularized expressions for the quark selfenergy and pion polarizations are presented. Some numerical results for the pion mass and effective coupling are discussed in Sec. 3, and the last section is devoted to drawing the conclusions.

## 2 Effects of the AMM on the vacuum properties in the NJL model

The SU(2) NJL model extended with an AMM term has the Lagrangian density

$$\mathcal{L}_{NJL} = \bar{\psi} \left( i\not{D} - M_0 - \frac{1}{2} \kappa \sigma_{\mu\nu} F^{\mu\nu} \right) \psi + G \left[ (\bar{\psi}\psi)^2 + (\bar{\psi}i\gamma^5\tau_a\psi)^2 \right],$$

where a summation over color and flavor is implicit and  $M_0$  stands for the degenerate current mass which explicitly breaks the chiral symmetry. The covariant derivative is written as  $D^\mu = \partial^\mu - iQeA^\mu/3$ , where  $Q = \text{diag}(2, -1)$  and a uniform magnetic field along the  $z$  axis is assumed. The definition  $\sigma_{\mu\nu} = i[\gamma_\mu, \gamma_\nu]/2$  is used and the AMM are displayed in the matrix  $\kappa = \text{diag}(\kappa_u, \kappa_d)$ . Each component can be written in terms of the dimensionless coefficient  $a_f$  as

$$\kappa_f = \frac{e Q_f}{6M_v} a_f \quad (1)$$

where  $M_v$  stands for the vacuum value of the constituent quark mass.

This interaction can be used in the mean field approach to evaluate the quark condensate that gives rise to the constituent mass, or to search for mesonic modes in a given quark - antiquark channel. The quark selfenergy as well as the pion polarization function can be evaluated using the appropriate quark propagator. The standard approach uses the Schwinger propagator, for a quasiparticle state dressed by the interaction with a uniform magnetic field. In the present work an expanded propagator is used which includes the coupling to the AMM [33].

$$G_f(x', x) = e^{i\Phi} \int \frac{d^4p}{(2\pi)^4} e^{-ip^\mu(x'_\mu - x_\mu)} e^{-p_\perp^2/\beta_f} \left[ G_{f0}(p) + \sum_{n,s} (-1)^n G_{fns}(p) \right] \quad (2)$$

where

$$G_{f0}(p) = (\not{p} + M_f \mp K_f) (1 \pm i\gamma^1\gamma^2) \Xi_{0s}, \quad (3)$$

$$\begin{aligned} G_{fns}(p) &= \frac{\Delta_n + sM_f}{2\Delta_n} \left\{ (\not{p} \mp K_f + s\Delta_n) (1 \pm i\gamma^1\gamma^2) L_n(2p_\perp^2/\beta_f) - (\not{p} \pm K_f - s\Delta_n) \right. \\ &\quad \times (1 \mp i\gamma^1\gamma^2) \frac{s\Delta_n - M_f}{s\Delta_n + M_f} L_{n-1}(2p_\perp^2/\beta_f) \pm (\not{p} i\gamma^1\gamma^2 \pm s\Delta_n - K_f) \not{p} \frac{s\Delta_n - M_f}{p_\perp^2} \\ &\quad \left. \times [L_n(2p_\perp^2/\beta_f) - L_{n-1}(2p_\perp^2/\beta_f)] \right\} \Xi_{ns}, \end{aligned} \quad (4)$$

$$\Xi_{ns} = \frac{1}{p_0^2 - E_{fns}^2 + i\epsilon} + 2\pi i \delta(p_0^2 - E_{fns}^2) n_F(p_0) \quad (5)$$

where

$$n_F(p_0) = \frac{\theta(p_0)}{1 + e^{(p_0 - \mu)/T}} - \frac{\theta(-p_0)}{1 + e^{-(p_0 - \mu)/T}}$$

The double signs distinguish between positively (upper) and negatively (lower) charged states. Furthermore, the index  $s = \pm 1$  describes the spin projection on the direction of the uniform magnetic field. Eq. (3) propagates the lowest Landau level with the unique projection  $s = 1$  for the  $u$  flavor and  $s = -1$  for the  $d$  case. The sum over the index  $n \geq 1$  takes account of the higher Landau levels, and the following notation is used  $\beta_f = e|Q_f|B/3$ ,

$K_f = \kappa_f B$ ,  $\not{d} = p_0\gamma^0 - p_z\gamma^3$ ,  $\not{d} = -p_x\gamma^1 - p_y\gamma^2$ ,  $p_\perp^2 = p_x^2 + p_y^2$ ,  $L_m$  stands for the Laguerre polynomial of order  $m$ , and

$$\begin{aligned} E_{fns} &= \sqrt{p_z^2 + (\Delta_n - sK_f)^2} \\ \Delta_n &= \sqrt{M_f^2 + 2n\beta_f} \end{aligned}$$

Clearly  $n_F(p_0)$  represents the canonical statistical distribution function for fermions in thermodynamical equilibrium. Finally, the phase factor  $\Phi = \beta_f(x + x')(y' - y)/2$  denotes the gauge fixing.

In the following subsections some specific details about the evaluation of the selfenergy and polarization functions are given.

Due to the presence of a vacuum condensate the quark field acquires an enlarged constituent mass, a process that in the usual mean field approach is described by

$$M_i = M_0 - 4G\langle\bar{\psi}_i\psi_i\rangle \quad (6)$$

The quark condensates can be evaluated using the quark propagator by using the formula [2]

$$\langle\bar{\psi}_f\psi_f\rangle = -i \lim_{t' \rightarrow t^+} \text{Tr}\{G_f(t, \vec{r}, t', \vec{r}')\}, \quad (7)$$

The right hand side is ultraviolet divergent and must be redefined properly. In [33], this author presented a result based on a simplifying assumption. As an improvement of such derivation, an exact expression is given here. Starting with

$$\langle\bar{\psi}_f\psi_f\rangle = -i \lim_{\epsilon \rightarrow 0^+} \int \frac{d^4p}{(2\pi)^4} \text{Tr}\{G_f(p)\} \quad (8)$$

a decomposition

$$\langle\bar{\psi}_f\psi_f\rangle = \langle\bar{\psi}_f\psi_f\rangle^{\text{vac}} + \langle\bar{\psi}_f\psi_f\rangle^{\text{F}} \quad (9)$$

is obtained. The first term in this equation corresponds to the vacuum contribution and it is generated by the first term of Eq. (5).

For practical purposes the integration is split into longitudinal  $d^2p_{\parallel} = dp_0 dp_z$  and orthogonal  $d^2p_{\perp} = dp_x dp_y$  components. After integrating over the perpendicular momentum one obtains

$$\langle\bar{\psi}_f\psi_f\rangle^{\text{vac}} = -\frac{i}{4\pi^3} N_c \beta_f M_f \left( \sum'_{n,s} \int \frac{d^2p_{\parallel}}{p_0^2 - E_{fns}^2 + i\epsilon} - K_f \sum'_{n,s} \frac{s}{\Delta_n} \int \frac{d^2p_{\parallel}}{p_0^2 - E_{fns}^2 + i\epsilon} \right) \quad (10)$$

where the primed sum indicates that for  $n = 0$  only one spin projection must be considered as already explained. Each of the terms between parenthesis can be evaluated by making a Wick rotation and introducing an auxiliary integration to bring the integrand into an exponential form. Thus, for instance

$$\begin{aligned} \sum'_{n,s} \int \frac{d^2p_{\parallel}}{p_0^2 - E_{fns}^2 + i\epsilon} &= -i\pi \lim_{\epsilon \rightarrow 0} \sum'_{n,s} \Gamma(\epsilon) \left[ \frac{\nu}{(\Delta_n - sK_f)^2} \right]^{\epsilon} \\ &= -i\pi \lim_{\epsilon \rightarrow 0} \left[ \left( \frac{1}{\epsilon} - \gamma \right) \frac{K_f^2 - M_f^2}{2\beta_f} + \ln \left( \frac{\Gamma(q_f)}{\sqrt{2\pi}} \right) + \frac{\beta_f + K_f^2 - M_f^2}{\beta_f} \ln \left( \frac{\nu}{2\beta_f} \right) + \ln \left( \frac{(M_f \pm K_f)^2}{\nu} \right) + O(\epsilon) \right] \end{aligned}$$

In this formula  $\nu$  represents a regularization scale parameter, which is fixed at  $\nu = M_f$ , and the definition  $q_f = (M_f^2 - K_f^2)/(2\beta_f)$  is used. The derivation of the second term is slightly more complex and is left for the Appendix A. The final result is

$$\sum'_{n,s} \frac{s}{\Delta_n} \int \frac{d^2 p_{\parallel}}{p_0^2 - E_{fns}^2 + i\epsilon} = -i\pi \lim_{\epsilon \rightarrow 0} \left\{ \frac{1}{\epsilon} \left( \frac{\pm 1}{M_f} + \frac{2K_f}{\beta_f} \right) \mp \frac{1}{M_f} \left[ \gamma + \ln \left( \frac{(M_f \pm K_f)^2}{\nu} \right) \right] + \frac{2K_f}{\beta_f} \ln \left( \frac{\nu}{2\beta_f} \right) - \frac{K_f}{\beta_f} \int_0^1 dx \left[ \psi(z) + \psi(z^*) + ix \frac{\psi(z) - \psi(z^*)}{\sqrt{1-x^2}} \right] + O(\epsilon) \right\} \quad (11)$$

where  $z = [M_f^2 + (1 - 2x^2)K_f^2 + i2x\sqrt{1-x^2}K_f^2]/2\beta_f$ . Taking account of the properties of the digamma function  $\psi$  on the complex plane, one can verify that the integrand in the last line is real and well defined, even for  $x = 1$ . Inserting the two last results into Eq. (10) one obtains

$$\langle \bar{\psi}_f \psi_f \rangle^{\text{vac}} = \frac{N_c}{(2\pi)^2} M_f \left[ \frac{1}{\epsilon} \left( M_f^2 + K_f^2 \pm \beta_f \frac{K_f}{M_f} \right) + \mathcal{F}(\beta_f, K_f, M_f) + O(\epsilon) \right] \quad (12)$$

The main term has a contribution  $M_f^3/(2\pi)^2$  coincident with the standard result of the NJL model at  $B = 0$ . In addition a contribution depending on  $B^2$  can be found. Using the fact that the main coefficient is a polynomial of degree two in  $B$ , a redefinition of the quark condensate is made before taking the limit  $\epsilon \rightarrow 0$

$$\langle \bar{\psi}_f \psi_f \rangle^{\text{reg}} = \langle \bar{\psi}_f \psi_f \rangle^{\text{vac}} - \left( 1 + \frac{K_f^2}{2} \frac{\partial^2}{\partial K_f^2} + \frac{K_f}{2} \beta_f \frac{\partial^2}{\partial \beta_f \partial K_f} \right) \langle \bar{\psi}_f \psi_f \rangle_{B=0}^{\text{vac}} \quad (13)$$

This expression is free of divergences and becomes zero for  $B = 0$ . Since one of the purposes of the regularization is to recover the phenomenology of the NJL model at zero magnetic intensity, a term  $\langle \bar{\psi}_f \psi_f \rangle^{\text{NJL}}$  corresponding to the standard result using the 3-momentum cutoff  $\Lambda$ , is added to (13). Thus, the final result is

$$\begin{aligned} \langle \bar{\psi}_f \psi_f \rangle^{\text{reg}} = \langle \bar{\psi}_f \psi_f \rangle^{\text{NJL}} &+ \frac{N_c}{(2\pi)^2} M_f \left\{ M_f^2 + 2\beta_f \ln \left( \frac{\Gamma(q_f)}{\sqrt{2\pi}} \right) + (\beta_f - K_f^2 - M_f^2) \ln \left( \frac{\nu}{2\beta_f} \right) \right. \\ &+ \beta_f \left( 1 \pm \frac{K_f}{M_f} \right) \ln \left( \frac{(M_f \pm K_f)^2}{\nu} \right) \\ &\left. + K_f^2 \int_0^1 dx \left[ \psi(z) + \psi(z^*) + ix \frac{\psi(z) - \psi(z^*)}{\sqrt{1-x^2}} \right] \right\} \quad (14) \end{aligned}$$

$$\langle \bar{\psi}_f \psi_f \rangle^{\text{NJL}} = \frac{N_c}{2\pi^2} M_f \left[ M_f^2 \ln \left( \frac{\Lambda + E_\Lambda}{M_f} \right) - \Lambda E_\Lambda \right] \quad (15)$$

The second term in Eq. (9) corresponds to the contribution of the Fermi sea of quarks. It is obtained straightforwardly by using the second term of Eq. (10). At zero temperature it is given by

$$\langle \bar{\psi}_f \psi_f \rangle^{\text{F}} = \frac{N_c}{2\pi^2} \beta_f M_f \sum'_{n,s} \frac{\Delta_n - sK_f}{\Delta_n} \ln \left( \frac{\mu_f + p_{fns}}{\Delta_n - sK_f} \right), \quad (16)$$

Where  $\mu_f$  stands for the chemical potential and the Fermi momentum is given by the condition  $\mu_f^2 = p_{fns}^2 + (\Delta_n - sK_f)^2$ . It must be noticed that at zero temperature the sum in Eq. (16) extends till the maximum value  $N$  wich satisfies the condition  $\mu_f^2 \geq (\Delta_n - sK_f)^2$ . Furthermore, if only the baryon number is conserved one must take  $\mu_u = \mu_d$ .

## 2.1 The pion polarization function

The pion is a Goldstone boson in the NJL model, therefore it does not have pre-existing dynamics and its properties must be defined ad-hoc. Mesonic excitations in a given quark-antiquark channel can be found by using the corresponding polarization insertion  $\Pi(q)$ . In particular the meson mass  $m$  is defined as the solutions of the equation [1, 3, 2]

$$1 - 2G\Pi(q^2 = m^2) = 0 \quad (17)$$

Usually the polarization is evaluated in the random phase approximation which sums up the ring diagram to all orders. Within this approach the polarization for the neutral pion can be written as

$$\Pi(q) = i \sum_f \int \frac{d^4p}{(2\pi)^4} \text{Tr} \{i\gamma_5 G_f(p) i\gamma_5 G_f(p-q)\}$$

In this work the pion properties are examined at zero temperature, for this purpose it is sufficient the quark propagator shown in Eqs.(2-5), with the fermion distribution function replaced by the step function  $n_F(p_0) = \Theta(\mu - p_0)$ . This propagator has been deduced for positively charged fermions in [48] within the thermal field theory known as Thermo Field Dynamics [49]. This is a real time formalism which duplicates its internal degrees of freedom in order to reproduce the main results and procedures of the field theory. Therefore the propagator becomes a  $2 \times 2$  matrix in the thermal space, the Eqs.(2-5) describe the (1,1) component of the matricial arrangement. To extend the present results to finite temperatures the full matrix structure must be considered.

As made for the quark condensate, the polarization can be decomposed as

$$\Pi(q) = \Pi^{\text{vac}}(q) + \Pi^{\text{F}}(q) \quad (18)$$

where the first term is obtained by using only the first term of Eq. (5) in both propagators. Since the Eq. (17) selects the time-like pion momentum, in the following  $q = 0$  is taken. This assumption eases the mathematical procedure, although it is not indispensable.

A detailed inspection of  $\Pi^{\text{vac}}$  shows that after using the expansion shown in Eq. (2) for both propagators, the integration over  $p_\perp$  cancels out the crossed terms  $G_{f0}G_{fn_s}$  because of the orthogonality of the Laguerre functions. The same integration carried out over terms of the form  $G_{fn_s}G_{fn's'}$  turns out proportional to  $\delta_{nn'}\delta_{ss'}$ . It deserves to be pointed out that even in the presence of the AMM the pion vertices do not mix different spin projections.

After these simplifications, one can write

$$\Pi_f^{\text{vac}}(q_0) = -\frac{i}{\pi} N_c \beta_f \sum'_{n,s} \left( \int \frac{d^2 p_\parallel}{p_0^2 - E_{fn_s}^2 + i\epsilon} - \frac{q_0^2}{2} \int d^2 p_\parallel (p_0^2 - E_{fn_s}^2 + i\epsilon)^{-1} \left[ (p_0 - q_0)^2 - E_{fn_s}^2 + i\epsilon \right]^{-1} \right) \quad (19)$$

The first term between parenthesis have been examined in the preceding section. The derivation of the second term is delegated to the Appendix B, and the final result is shown here

$$\begin{aligned} \sum'_{n,s} \int \frac{d^2 p_\parallel}{(p_0^2 - E_{fn_s}^2 + i\epsilon) \left[ (p_0 - q_0)^2 - E_{fn_s}^2 + i\epsilon \right]} &= i\pi \lim_{\epsilon \rightarrow 0} \left\{ \frac{1}{\epsilon} \frac{1}{\beta_f} + 2 \ln \left( \frac{\nu}{2\beta_f} \right) + \int_0^1 \frac{dx}{q_0^2 x(1-x) - (M_f \pm K_f)^2} \right. \\ &\quad \left. - \frac{1}{2\beta_f} \left[ \psi(q_+) + \psi(q_-) + \frac{K_f}{q_0} \frac{\psi(q_+) - \psi(q_-)}{\sqrt{x(1-x)}} \right] + O(\epsilon) \right\} \quad (20) \end{aligned}$$

where

$$q_{\pm} = \frac{M_f^2 - [K_f \pm x(1-x)q_0]^2}{2\beta_f} \quad (21)$$

Collecting these partial results together one obtains

$$\Pi^{\text{vac}}(q_0) = -\frac{N_c}{(2\pi)^2} \left[ \frac{1}{\epsilon} \left( \frac{q_0^2}{2} - M_f^2 + K_f^2 \right) + \mathcal{G}(\beta_f, K_f, M_f, q_0) + O(\epsilon) \right] \quad (22)$$

The main coefficient presents the same kind of divergence  $(q_0^2 - 2M_f^2)/8\pi^2$  as the usual result at  $B = 0$ , complemented with a contribution explicitly depending on  $B^2$ . Applying the regularization program described at the end of the preceding section, i.e.

$$\Pi^{\text{reg}}(q_0) = \Pi^{\text{NJL}}(q_0) + \Pi^{\text{vac}}(q_0) - \left( 1 + \frac{K_f^2}{2} \frac{\partial^2}{\partial K_f^2} \right) \Pi_{B=0}^{\text{vac}} \quad (23)$$

one finally obtains

$$\begin{aligned} \Pi^{\text{reg}}(q_0) &= \Pi^{\text{NJL}}(q_0) - \frac{N_c}{4\pi^2} \left\{ M_f^2 + 2\beta_f \ln \left( \frac{\Gamma(q_f)}{\sqrt{2\pi}} \right) + \left( \beta_f + K_f^2 - M_f^2 + \frac{q_0^2}{2} \right) \ln \left( \frac{\nu}{2\beta_f} \right) + \beta_f \ln \left( \frac{(M_f \pm K_f)^2}{\nu} \right) \right. \\ &+ \frac{q_0^2}{2} \left[ \beta_f \int_0^1 \frac{dx}{q_0^2 x(1-x) - (M_f \pm K_f)^2} + \int_0^1 dx \ln \left( \frac{M_f^2 - q_0^2 x(1-x)}{\nu} \right) - \frac{1}{2} \int_0^1 dx [\psi(q_+) + \psi(q_-)] \right] \\ &\left. + K_f \frac{q_0}{4} \int_0^1 dx \frac{\psi(q_-) - \psi(q_+)}{\sqrt{x(1-x)}} \right\} \quad (24) \end{aligned}$$

$$\Pi^{\text{NJL}}(q_0) = -\frac{N_c}{\pi^2} \int_0^\Lambda dp p^2 \frac{\sqrt{p^2 + M_f^2}}{p^2 + M_f^2 - q_0^2/4} \quad (25)$$

The last piece is the Fermi sea contribution to the polarization, which at zero temperature is given by

$$\Pi_f^F(q_0) = \frac{\beta_f}{2\pi^2} \sum'_{n,s} \int_0^{p_{fns}} dp \frac{\sqrt{p^2 + M_f^2}}{p^2 + M_f^2 - q_0^2/4} \quad (26)$$

Some imaginary terms giving zero contribution within the regime considered in the present work have been omitted.

The pion mass  $m$  found as a solution of Eq. (17) gives the ground energy of this bound state. A measure of how this state interacts with its environment can be obtained by the effective coupling. The strength  $g_{\pi q}$  of the coupling of a pion with a pair quark-antiquark can be obtained as [2]

$$g_{\pi q}^{-2} = \frac{\partial}{\partial q_0^2} \Pi \Big|_{q_0=m}. \quad (27)$$

### 3 Results and discussion

In this section the effects of the AMM in the mass of the pion and its coupling to quarks are studied in terms of the magnetic intensity and the baryonic number density.



In the present calculations the NJL parameters corresponding to the set 2 of Ref. [4] are used,  $M_0 = 5.6$  MeV,  $\Lambda = 587.9$  MeV,  $G = 2.44/\Lambda^2$ . Taking as a guide the prescriptions  $\mu_u = (4\mu_p + \mu_n)/5$ ,  $\mu_d = (\mu_p + 4\mu_n)/5$  of the constituent quark model together with the experimental values of the proton and neutron magnetic moments one can find a plausible range for the AMM. For illustrative purposes two sets are considered in the present work. For the set AMM1 the numerical values  $\kappa_u = 0.074\mu_N$ ,  $\kappa_d = 0.127\mu_N$ , expressed in units of the nuclear magneton, are chosen. Using  $M_v = 400$  MeV as given in the present parametrization [4], the coefficients  $a_f = 0.05, 0.16$  are obtained, see Eq. (1). Motivated by theoretical estimations [36, 37], the considerably stronger values  $\kappa_u = \kappa_d = 0.38\mu_N$  are included in the alternative set AMM2. They correspond to  $a_f = 0.24, 0.48$ , which is compatible with the results of [37].

For given values of  $B$  and the baryon density, first the quark masses must be solved in a self-consistent way. The different electric charge of the  $u$  and  $d$  flavors inevitably leads to a breakdown of the isospin symmetry which is enhanced for higher  $B$ . This, in turn, produce a mixing of the pion with other meson states, as for instance kaons and  $\eta - \eta'$ . To avoid such complication some studies use an averaged quark condensate and a degenerate quark mass. That is, Eq.(6) is replaced by

$$M_u = M_d = M_{\text{symm}} = M_0 - 4G \left( \frac{1}{2} \sum_f \langle \bar{\psi}_f \psi_f \rangle^{\text{reg}} \right) \quad (28)$$

To test the effects of using as input for the solutions of Eq.(17) either the symmetrized (28) or the non-degenerate quark mass (6) both results are compared in Fig.1 for the case AMM1. The results correspond to zero baryon density and a wide range of intensities. For  $B < 2.5 \times 10^{19}$  G the discrepancy is negligible. For stronger fields the symmetrized case gives an almost linear response. The highest difference is achieved at the end of the scale, representing a 5% of deviation. Due to this small difference, in the following the non degenerate flavor approach is adopted since it also will make evident the need of new physical input. A full treatment including meson mixing is pending.

The behavior of the pion mass as a function of the intensity  $B$  is shown in Fig. 2, for zero baryon density and different values for the AMM. All the results coincide in the very low intensity regime because of the regularization prescription. For intermediate magnitudes  $B < 3 \times 10^{19}$  G the calculations with zero AMM (labelled as AMM0) and using the set AMM1 are comparable, while the AMM2 case is clearly different. For very strong fields, the AMM0 curve shows a decrease until  $B \simeq 1.2 \times 10^{20}$  G where a slow increase starts. This behavior is compatible with the predictions of [28, 44]. The outcomes of the AMM1 and AMM2 sets are definitely decreasing functions of  $B$ . A monotonously decreasing pion mass has also been obtained in the framework of the linear sigma model under the strong field treatment of [44], when dressed couplings are used. This parameters are obtained at the one-loop level using the Schwinger propagator [50] and hence they acquire  $B$  dependency. However the decreasing rate is lesser than that in the AMM1 case. The parametrization AMM2 yields the unexpected combination of increasing quark masses and collapsing pion mass.

These qualitative differences can only be ascribed to the input of quark masses provided for each set of AMM. In Fig. 3 the dependence on the intensity  $B$  is shown for the deviation of the symmetrized mass (upper panel)

$$\Delta M = \frac{M_u + M_d}{2} - M_{\text{symm}}$$

and the flavor dispersion  $M_u - M_d$  (lower panel) of the quark masses. It is evident that the AMM3 case has the greatest rate of growth of the flavor splitting, together with the more rapid deviation from the symmetrized value. An immediate conclusion is that the behavior of the in-vacuum pion mass strongly depends on the rate at which the magnetic intensity affects the flavor symmetry.

In the next figure, the effective coupling of the neutral pion to the quark-antiquark pair is shown in terms of

the intensity  $B$ . Results from the AMM0 case are in good agreement with the findings of [28]. The set AMM3 distinguishes again from the other cases keeping slightly below its value for  $B = 0$ .

At this point some remarks about the neutral scalar excitation or  $\sigma$  meson are appropriate. In contrast to the pion vertex, the scalar one allows the mix of different spin projections, which in the presence of AMM would result in a non-trivial structure. Furthermore a regularization program in terms of the zeta function will conclude probably with digamma functions of arguments as shown in Eq.(21). Taking into account that the sigma meson mass verifies  $M^2 - m_\sigma^2/4 < 0$  for most of the NJL parametrizations, one can expect that  $q_\pm$  crosses from positive to negative values as  $x$  varies in  $[0, 1]$ . This implies that the digamma function would cross some of its poles as the integration is carried out. This remark holds even for zero AMM.

The remaining of this section is devoted to the discussion of the finite baryon density effects in combination with the magnetism. It is usual to analyze indirectly these effects by introducing the associated chemical potential  $\mu$ . However most of the given range of variation  $\mu < M_f$  reproduce the same state of vacuum. In this work a different strategy is adopted by recursing to the isospin conservation [51, 52]. Two particular configurations will be considered, symmetric matter, where the Fermi sea is populated with equal number of each flavor  $N_u = N_d$ , and electrically neutral matter where  $2N_u = N_d$ . They are schematic descriptions of definite physical situations as found in heavy ion collisions experiences or in quark stars, respectively. The simultaneous conservation of baryon and isospin charges can be expressed by independent chemical potentials for each flavor. In Fig. 5 the mass of a pion immersed in dense symmetric matter is shown as a function of the background magnetic intensity. Three different values of the baryon number density are considered  $n/n_0 = 0.5, 1, 1.5$ , where  $n_0 = 0.15 \text{ fm}^{-3}$  represents the equilibrium density of the nuclear matter. For very low  $B$ , an increase in density yields an enhancement of the pion mass as expected for calculations with flavor asymmetry [53, 54]. For the set AMM0 the density effects are neutralized by the increase of the magnetic intensity, since after a slow decrease all the curves corresponding to different densities coalesce into the same behavior. This is not the case when the AMM are considered. As can be seen in the panels (b) and (c) as the density grows the decreasing trend in the high density regime is emphasized. Thus, for  $n/n_0 = 1.5$  the set AMM1 predicts a collapse of the pion mass for  $B \simeq 7 \times 10^{19} \text{ G}$ . As already seen, the set AMM2 yields a massless pion even at zero density for strong enough intensities. This threshold intensities are  $B \simeq 6, 5$  and  $3.7 \times 10^{19} \text{ G}$  for  $n/n_0 = 0, 0.5$  and  $1$ , respectively. For  $n/n_0 = 1.5$  the curve for the pion mass ends abruptly near  $B \simeq 2.5 \times 10^{19} \text{ G}$  because the solutions for the quark masses cease to exist.

In Fig. 6 the density effects are analyzed for a configuration of electrically neutral matter. With the motivation of the high densities achieved in compact quark stars, which satisfy this requisite, an extended range of densities  $n/n_0 < 3$  is considered. The general trend is similar as that described in Fig. 5, but in this case for given values of  $n, B$  the pion mass is slightly above than in the previous case.

It is interesting to note that under specific circumstances the magnetic field acts as an stabilizer for the pion field. It is well known that the pion becomes unstable as the condition  $M - m/2 < 0$  is reached. For  $B = 0$  an increase in density yields an increase of  $m$ , which favors the instability. In contrast, for a given density  $m$  decreases with  $B$ . The situation is sketched in Fig. 7, corresponding to the  $n_d = 2n_u$  at fixed density  $n/n_0 = 4$ . The dashed line corresponds to the threshold condition  $m = 2M$ , therefore the region above this curve corresponds to unstable states. As  $B$  grows the system leaves this region and the pion becomes stable. The same behavior is found for the cases AMM0 (upper panel) and AMM1 (lower panel).

The effective coupling of the pion is revisited in Fig.8 as a function of  $B$  but for fixed density  $n/n_0 = 3$  using the  $n_d = 2n_u$  configuration. The finite density produces drastic changes as compared to Fig. 4, there is a general enhancement for all the range of  $B$ , indicating a stronger correlation in dense matter. There is a clearly defined low  $B$  regime showing quick variations which are produced by the occupation of different Landau levels in Eq. (26). As the intensity grows the upper Landau levels are drained and for instance in the AMM0 case, the  $u$  flavor is completely polarized at  $B \simeq 1.7 \times 10^{19} \text{ G}$ . This fact is manifested by the highest peak in the curve.

The  $d$  flavor continues partially polarized until  $B \simeq 2.5 \times 10^{19}$  G where it is confined to the lowest Landau level. At this point  $g_{\pi q}$  has its last abrupt drop and enters in a slow regime, first decreasing and finally monotonously increasing. A similar description holds for the AMM1 set.

## 4 Summary and Conclusions

In this work some basic properties of the neutral pion immersed in a background magnetic field are studied, when non-zero anomalous magnetic moments are assumed for the constituent quarks. For this purpose the pion polarization function is evaluated in the random phase approximation using the SU(2) version of the NJL model supplemented with linear couplings between the external field and the AMM. Recent publications have warned about the use of an appropriate regularization of the NJL model in the presence of an external field to avoid spurious results in physical observables. In the present calculations it has been shown that the AMM gives rise to additional divergences depending on the magnetic intensity, which need an adequate treatment. In consequence an analytical regularization procedure is proposed to isolate unambiguously this kind of singularities and to eliminate its effects on the quark condensate and the pion polarization. As an extra requisite the regularization used converges to the standard NJL treatment as  $B$  goes to zero.

The calculations have been made by using a covariant propagator for the quarks with constituent mass, which takes account of the full effect of the magnetic field as well as the effect of the AMM.

The regularized model has been used to study the pion mass  $m$  and effective coupling  $g_{\pi q}$ , taking the magnetic intensity and the baryon density as variables. The description of dense matter have been made assuming isospin conservation and taking as examples two configurations, flavor symmetric and electrically neutral quark matter. Two sets of phenomenological AMM are chosen of different magnitude. the weak (AMM1) and strong (AMM2) sets. A wide range of magnetic intensities  $B < 10^{20}$  G and densities up to three times the normal nuclear matter value were analyzed.

The inclusion of the AMM changes the behavior of the pion mass for strong fields, giving a decreasing trend for sufficiently high intensity. Under some circumstances this could lead to the collapse of the pion mass, particularly for the set AMM2. This result is emphasized as the baryon density is increased. It has been found that density and magnetism have opposite effects on the stability of the pion field in dense matter with isospin conservation. While a density increase favors the instability, the magnetic intensity has an stabilizing role by decreasing  $m$ .

The effective pion-quark coupling shows an increase of the correlation in the strong field regime for the vacuum in the AMM1 set. The opposite trend was found for the AMM2 case. The pion-quark interaction is strengthened in dense matter, and the effective coupling  $g_{\pi q}$  gives evidence of the population of the different Landau levels as  $B$  is varied.

For a restricted set  $B < 2 \times 10^{19}$  G, higher than the intensities produced in heavy ion collision experiments, both AMM1 and AMM2 sets provide acceptable results. However when the full range of intensities studied here is considered, the case AMM2 shows some features which make it less eligible.

This is a first approach that needs improvement, as for instance the inclusion of the mixing with other meson states in the calculation of the polarization function.

## 5 Appendix A: Derivation of Eq. (11)

As a first step, the primed summation in the second term on the right hand side of Eq. (10) is completed by summing and subtracting the same term

$$\begin{aligned} \sum'_{n,s} \frac{s}{\Delta_n} \int \frac{d^2 p_{\parallel}}{u_p^2 - (\Delta_n - sK_f)^2 + i\epsilon} &= \sum_n \int \frac{d^2 p_{\parallel}}{\Delta_n} \left[ \frac{1}{u_p^2 - (\Delta_n - K_f)^2 + i\epsilon} - \frac{1}{u_p^2 - (\Delta_n + K_f)^2 + i\epsilon} \right] \\ &\pm \frac{1}{M} \int \frac{d^2 p_{\parallel}}{u_p^2 - (m \pm K)^2 + i\epsilon} \end{aligned} \quad (29)$$

The right hand side can be rewritten after a Wick rotation as

$$-2iK_f \sum_n \int \frac{d^2 p_E}{u_E^2 + \Delta_n^2 + K_f^2} \left[ \frac{1}{u_E^2 + (\Delta_n - K_f)^2} + \frac{1}{u_E^2 + (\Delta_n + K_f)^2} \right] \mp \frac{i}{\nu M_f} \int \frac{d^2 p_E \nu}{u_E^2 + (m \pm K)^2} \quad (30)$$

where  $d^2 p_E = dp_z dp_4$  and  $u_E^2 = p_z^2 + p_4^2$ . Furthermore an undetermined scale constant  $\nu$  has been introduced. In the first term one can apply the following relation to each term between square brackets

$$\frac{1}{AB} = \int_0^1 \frac{dx}{[xA + (1-x)B]^2} \quad (31)$$

to obtain

$$-2iK_f \sum_{n,s=\pm 1} \int d^2 p_E \int_0^1 \frac{dx}{[u_E^2 + \Delta_n^2 + K_f^2 + 2xsK_f\Delta_n]^2} \mp \frac{i}{\nu M_f} \int \frac{d^2 p_E \nu}{u_E^2 + (m \pm K)^2} \quad (32)$$

At this point an integration over the auxiliary variable  $\tau$  is introduced to bring the integrands into an exponential form, which allows an easy integration over  $d^2 p_E$  yielding

$$-2\pi i K_f \sum_{n,s=\pm 1} \int_0^1 dx \int_0^\infty d\tau \exp[-\tau(\Delta_n^2 + K_f^2 + 2xsK_f\Delta_n)] \mp \frac{i\pi}{\nu M_f} \int_0^\infty \frac{d\tau}{\tau} \exp[-\tau(M_f \pm K_f)^2/\nu] \quad (33)$$

The integration in the first term is easily done and after some algebra the last equation takes the form

$$\begin{aligned} -2\pi i K_f \sum_n \int_0^1 \frac{dx}{\nu} &\left\{ \frac{\nu}{[\Delta_n^2 + (1-2x^2 + 2ix\sqrt{1-x^2})K_f^2]^{1+\epsilon}} + \frac{\nu}{[\Delta_n^2 + (1-2x^2 - 2ix\sqrt{1-x^2})K_f^2]^{1+\epsilon}} \right. \\ &+ \left. \frac{ix}{\sqrt{1-x^2}} \left( \frac{\nu}{[\Delta_n^2 + (1-2x^2 + 2ix\sqrt{1-x^2})K_f^2]^{1+\epsilon}} - \frac{\nu}{[\Delta_n^2 + (1-2x^2 - 2ix\sqrt{1-x^2})K_f^2]^{1+\epsilon}} \right) \right\} \\ &\mp \frac{i\pi}{M_f} \int_0^\infty d\tau \tau^{-1+\epsilon} \exp[-\tau(M_f \pm K_f)^2/\nu] \end{aligned} \quad (34)$$

After finishing the algebra an infinitesimal parameter  $\epsilon \rightarrow 0$  is introduced in order to isolate the singularity of both integrals. Remembering that  $\Delta_n^2 = 2\beta_f n + M_f^2$  and using the definitions of the gamma and the Hurwitz zeta functions, one finds

$$-\pi i \frac{K_f}{\beta_f} \left( \frac{\nu}{2\beta_f} \right)^\epsilon \int_0^1 dx \left\{ \zeta(1+\epsilon, z) + \zeta(1+\epsilon, z^*) + \frac{ix}{\sqrt{1-x^2}} [\zeta(1+\epsilon, z) - \zeta(1+\epsilon, z^*)] \right\} \mp \frac{i\pi}{M_f} \Gamma(\epsilon) \left[ \frac{\nu}{(M_f \pm K_f)^2} \right]^\epsilon$$

where the definition of  $z$  is given immediately after Eq. (11).

After making a Laurent expansion around  $\epsilon = 0$  and arranging according to same order of  $\epsilon$  one finally obtains the desired Eq. (11).

Use of the relation

$$\zeta(1 + \epsilon, z) = \frac{1}{\epsilon} - \psi(z) + O(\epsilon)$$

has been made.

## 6 Appendix B: Derivation of Eq. (20)

To start the Feynman propagators are replaced by its Euclidean version and then the relation (31) is used to rewrite the integrand

$$\begin{aligned} i \sum'_{n,s} & \int \frac{d^2 p_E}{\left[ u_{pE}^2 + (\Delta_n - sK_f)^2 \right] \left[ u_{(p-q)E}^2 + (\Delta_n - sK_f)^2 \right]} \\ & = i \sum'_{n,s} \int d^2 p_E \int_0^1 dx \left\{ [u_{pE} - (1-x)u_{qE}]^2 + (\Delta_n - sK_f)^2 + x(1-x)u_{qE}^2 \right\}^{-2} \end{aligned} \quad (35)$$

After introducing an integration over the auxiliary variable  $\tau$  one gets

$$\begin{aligned} i \sum'_{n,s} \int d^2 p_E \int_0^1 dx \int_0^\infty d\tau \tau \exp -\tau \left\{ [u_{pE} - (1-x)u_{qE}]^2 + (\Delta_n - sK_f)^2 + x(1-x)u_{qE}^2 \right\} \\ = i \sum'_{n,s} \int_0^1 dx \int_0^\infty d\tau \exp \left\{ -\tau [(\Delta_n - sK_f)^2 + x(1-x)u_{qE}^2] \right\} = i \pi \sum'_{n,s} \int_0^1 \frac{dx}{(\Delta_n - sK_f)^2 + x(1-x)u_{qE}^2} \end{aligned}$$

As the next step a return to the Minkowski space is made, and then to modify the summation the same term is added and subtracted

$$\begin{aligned} i \pi \int_0^1 dx \left\{ \frac{-1}{(M_f \pm K_f)^2 - x(1-x)u_q^2} + \sum_n \left[ \frac{1}{(\Delta_n - K_f)^2 - x(1-x)u_q^2} + \frac{1}{(\Delta_n + K_f)^2 - x(1-x)u_q^2} \right] \right\} \\ = -i \pi \int_0^1 \frac{dx}{(M_f \pm K_f)^2 - x(1-x)u_q^2} + i \pi \sum_n \int_0^1 dx \left\{ \frac{1}{[\Delta_n^2 - (K_f + q_0 w)^2]^{1+\epsilon}} + \frac{1}{[\Delta_n^2 - (K_f - q_0 w)^2]^{1+\epsilon}} \right. \\ \left. + \frac{K_f}{w q_0} \left[ \frac{1}{[\Delta_n^2 - (K_f + q_0 w)^2]^{1+\epsilon}} - \frac{1}{[\Delta_n^2 - (K_f - q_0 w)^2]^{1+\epsilon}} \right] \right\} \end{aligned} \quad (36)$$

After completing the algebra inside the summation, an infinitesimal parameter  $\epsilon \rightarrow 0$  is introduced in order to isolate the singularities. Furthermore the abbreviation  $w = \sqrt{x(1-x)}$  was defined. Using that  $\Delta_n^2 = 2\beta_f n + M_f^2$  and recursing to the definition of the Hurwitz zeta function, one finds

$$\begin{aligned} i \frac{\pi}{2\beta_f} \left( \frac{\nu}{2\beta_f} \right)^\epsilon \int_0^1 dx \left\{ \zeta(1 + \epsilon, q_+) + \zeta(1 + \epsilon, q_-) + \frac{K_f}{w q_0} [\zeta(1 + \epsilon, q_+) - \zeta(1 + \epsilon, q_-)] \right\} \\ - i \pi \int_0^1 \frac{dx}{(M_f \pm K_f)^2 - x(1-x)u_q^2} \end{aligned} \quad (37)$$

Where  $q_{\pm}$  are defined by Eq. (21).

Finally by making a Laurent expansion around  $\epsilon = 0$  and collecting terms of the same order in  $\epsilon$  one obtains the desired Eq. (20).

## Acknowledgements

This work has been partially supported by a grant from the Consejo Nacional de Investigaciones Cientificas y Tecnicas, Argentina under grant PIP 11220150100616CO.

## References

- [1] U. Vogl, W. Weise, Prog. Part. Nucl. Phys. **27**, 195 (1991).
- [2] S. P. Klevansky, Rev. Mod. Phys. **64**, 649 (1992).
- [3] T. Hatsuda, T. Kunihiro, Phys.Rept. **247**, 221 (1994).
- [4] M. Buballa, Phys.Rept. **407**, 205 (2005).
- [5] V. A. Miransky, I. A. Shovkovy, Phys. Rept. **576**, 1 (2015).
- [6] J. O. Andersen, W. R. Naylor, A. Tranberg, Rev. Mod. Phys. **88**, 025001 (2016).
- [7] V. P. Gusynin, V.A. Miransky, I.A. Shovkovy, Phys.Lett. B **349**, 477 (1995).
- [8] D. Ebert, K. G. Klimenko, M. A. Vdovichenko, A. S. Vshivtsev, Phys. Rev. D **61**, 025005 (1999).
- [9] E. J. Ferrer, V. de la Incera, C. Manuel, Nucl.Phys. B **747**, 88 (2006).
- [10] J. L. Noronha, I. A. Shovkovy, Phys.Rev. D **76**, 105030 (2007).
- [11] I.E. Frolov, V.Ch. Zhukovsky, K.G. Klimenko, Phys.Rev. D **82**, 076002 (2010).
- [12] B. Chatterjee, H. Mishra, A. Mishra, Phys.Rev. D **84**, 014016 (2011).
- [13] R. Z. Denke, M. B. Pinto, Phys.Rev. D **88**, 056008 (2013).
- [14] E. J. Ferrer, V. de la Incera, I. Portillo, M. Quiroz, Phys.Rev. D **89**, 085034 (2014).
- [15] A. Abhishek, H. Mishra, Phys.Rev. D **99**, 054016 (2019).
- [16] C. A. Islam, A. Bandyopadhyay, P. K. Roy, S. Sarkar, Phys.Rev. D **99**, 094028 (2019).
- [17] S. Ghosh, V. Chandra, Eur. Phys. J. A **56**, 190 (2020).
- [18] S. K. Blau, M. Visser, A. Wipf, Int. J. Mod. Phys. A **6**, 5409 (1991).
- [19] A. Goyal, M. Dahiya, Phys.Rev. D **62**, 025022 (2000).
- [20] J. O. Andersen, R. Khan, Phys.Rev. D **85**, 065026 (2012).
- [21] T. D. Cohen, E. S. Werbos, Phys.Rev. C **80**, 015203 (2009).

- [22] M. Ruggieri, M. Tachibana, V. Greco, *JHEP* **1307**, 165 (2013).
- [23] M. Coppola, D. Gomez Dumm, S. Noguera, N. N. Scoccola, *Phys. Rev. D* **100**, 054014 (2019).
- [24] D.P. Menezes, M. Benghi Pinto, S.S. Avancini, A. Perez Martinez, C. Providencia, *Phys.Rev. C* **79**, 035807 (2009).
- [25] Sh. Fayazbakhsh, S. Sadeghian, N. Sadooghi, *Phys.Rev. D* **86**, 085042 (2012).
- [26] A. Amador, J. O. Andersen, *Phys.Rev. D* **88**, 025016 (2013).
- [27] S. S. Avancini, V. Dexheimer, R. L. S. Farias, V. S. Timoteo, *Phys. Rev. C* **97**, 035207 (2018).
- [28] S. S. Avancini, W. R. Tavares, M. B. Pinto, *Phys. Rev. D* **93**, 014010 (2016).
- [29] S. S. Avancini, R. L. S. Farias, W. R. Tavares, *Phys. Rev. D* **99**, 056009 (2019).
- [30] S. S. Avancini, R. L.S. Farias, N. N. Scoccola, W. R. Tavares, *Phys.Rev. D* **99**, 116002 (2019).
- [31] Sh. Fayazbakhsh, N. Sadooghi, *Phys.Rev. D* **90**, 105030 (2014).
- [32] N. Chaudhuri, S. Ghosh, S. Sarkar, P. Roy, *Phys. Rev. D* **99**, 116025 (2019).
- [33] R. M. Aguirre, *Phys. Rev. D* **102**, 096025 (2020).
- [34] S. Ghosh, A. Mukherjee, N. Chaudhuri, P. Roy, S. Sarkar, *Phys. Rev. D* **101**, 056023 (2020).
- [35] J. P. Singh, *Phys.Rev. D* **31**, 1097 (1985).
- [36] Pedro J. de A. Bicudo, J. E. Ribeiro, R. Fernandes, *Phys. Rev. C* **59**, 1107 (1999).
- [37] M. Mekhfi, *Phys.Rev. D* **72**, 114014 (2005).
- [38] L.Chang, Y. X. Liu, C. D. Roberts, *Phys. Rev. Lett.* **106**, 072001 (2011).
- [39] S. Mao, D. H. Rischke, *Phys. Lett. B* **792**, 149 (2019).
- [40] J. Mei, S. Mao, *Phys. Rev. D* **102**, 114035 (2020).
- [41] R. G. Felipe, A. Perez Martinez, H. Perez Rojas, M. Orsaria, *Phys.Rev. C* **77**, 015807 (2008).
- [42] A. Mishra, A. K. Singh, N. S. Rawat, P. Aman, *Eur. Phys. J. A* **55**, 107 (2019).
- [43] A. Mukherjee, S. Ghosh, M. Mandal, P. Roy, S. Sarkar, *Phys. Rev. D* **96**, 016024 (2017).
- [44] A. Ayala, R. L. S. Farias, S. Hernández-Ortiz, L. A. Hernández, D. M. Paret, R. Zamora, *Phys. Rev. D* **98**, 114008 (2018); A. Ayala, J. L. Hernández, L. A. Hernández, R. L. S. Farias, R. Zamora; *Phys. Rev. D* **103** 054038 (2021).
- [45] A.Das, N.Haque, *Phys. Rev. D* **101**, 074033 (2020).
- [46] Z. Wang, P.Zhuang, *Phys. Rev. D* **97**, 034026 (2018).
- [47] H. Liu, X. Wang, L. Yu, M. Huang, *Phys. Rev. D* **97**, 076008 (2018).

- [48] R. M. Aguirre, A. L. De Paoli, Eur. Phys. J. A **52** 343 (2016).
- [49] N.P. Landsman, C.G. van Weert, Phys. Rept. **145** 141 (1987).
- [50] A. Ayala, J. L. Hernández, L. A. Hernández, R. L. S. Farias, R. Zamora, Phys. Rev. D **102**, 114038 (2020).
- [51] K. Splittorff, D. T. Son, M. A. Stephanov, Phys. Rev. D **64**, 016003 (2001).
- [52] B. Freedman, L. D. McLerran, Phys. Rev. D **17**, 1109 (1978).
- [53] C. A. de Sousa, M. C. Ruivo, Nucl. Phys. A **625**, 713 (1997).
- [54] P. Costa, M. C. Ruivo, Y. L. Kalinovsky, C. A. de Sousa, Phys. Rev. C **70**, 025204 (2004).



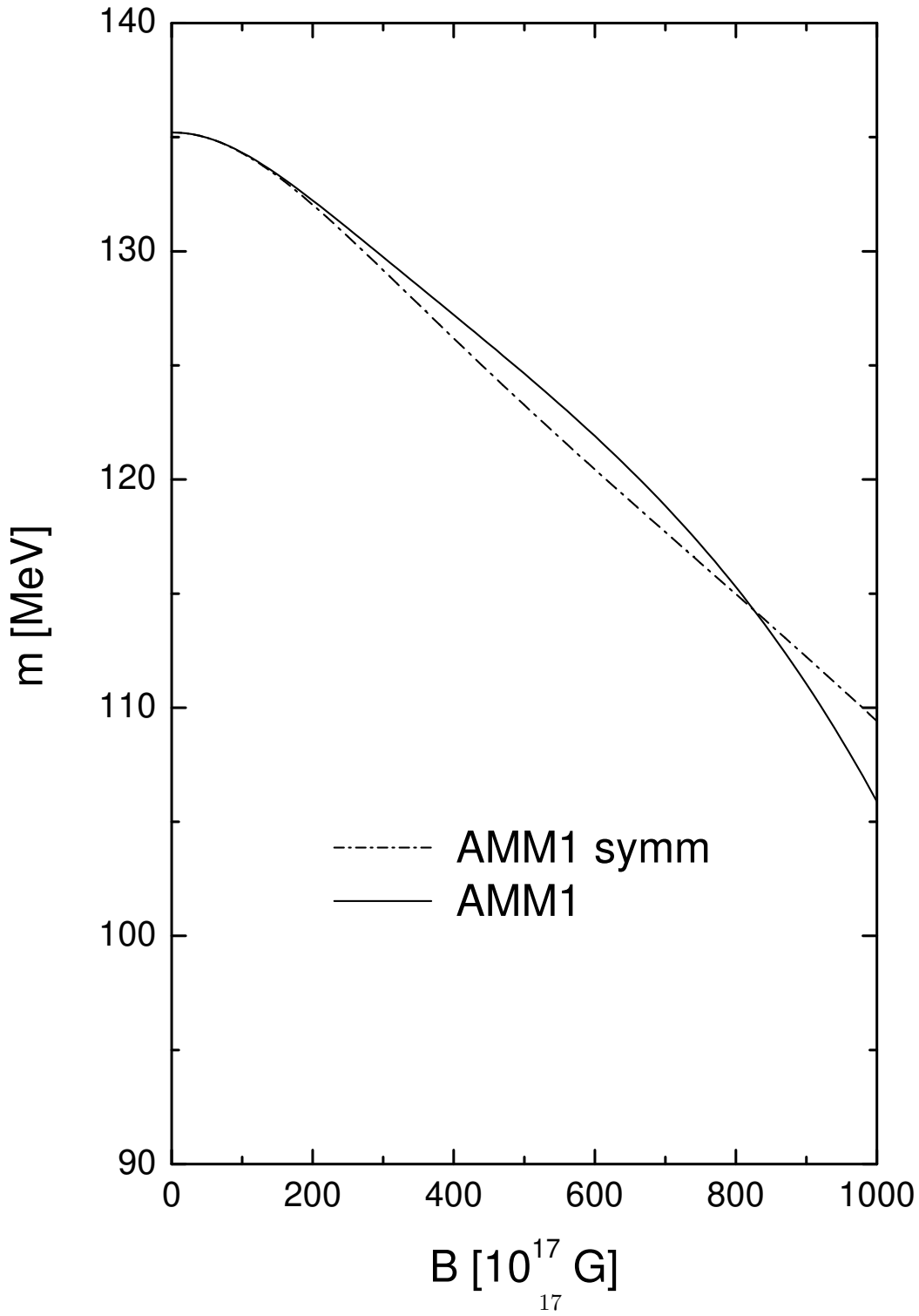


Figure 1: The in vacuo pion mass using the set AMM1 as a function of the magnetic intensity. Two results using as input a degenerate symmetrized quark mass  $M_{symm}$  defined by Eq.(28) or the non degenerate  $M_u \neq M_d$  case are shown.

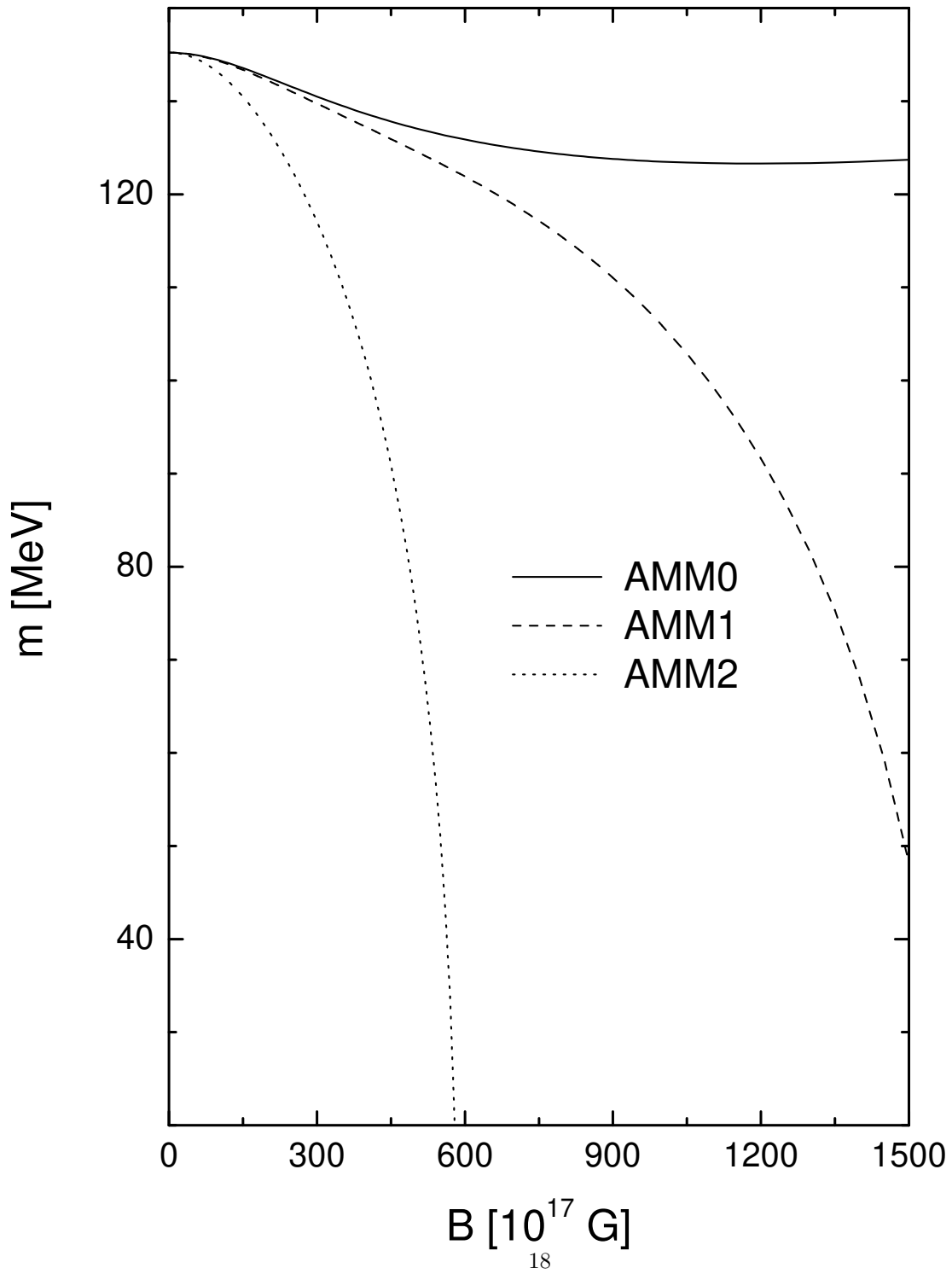


Figure 2: The in vacuum pion mass as a function of the magnetic intensity. The results without AMM (AMM0) and two different sets of AMM (AMM1 and AMM2) are compared.

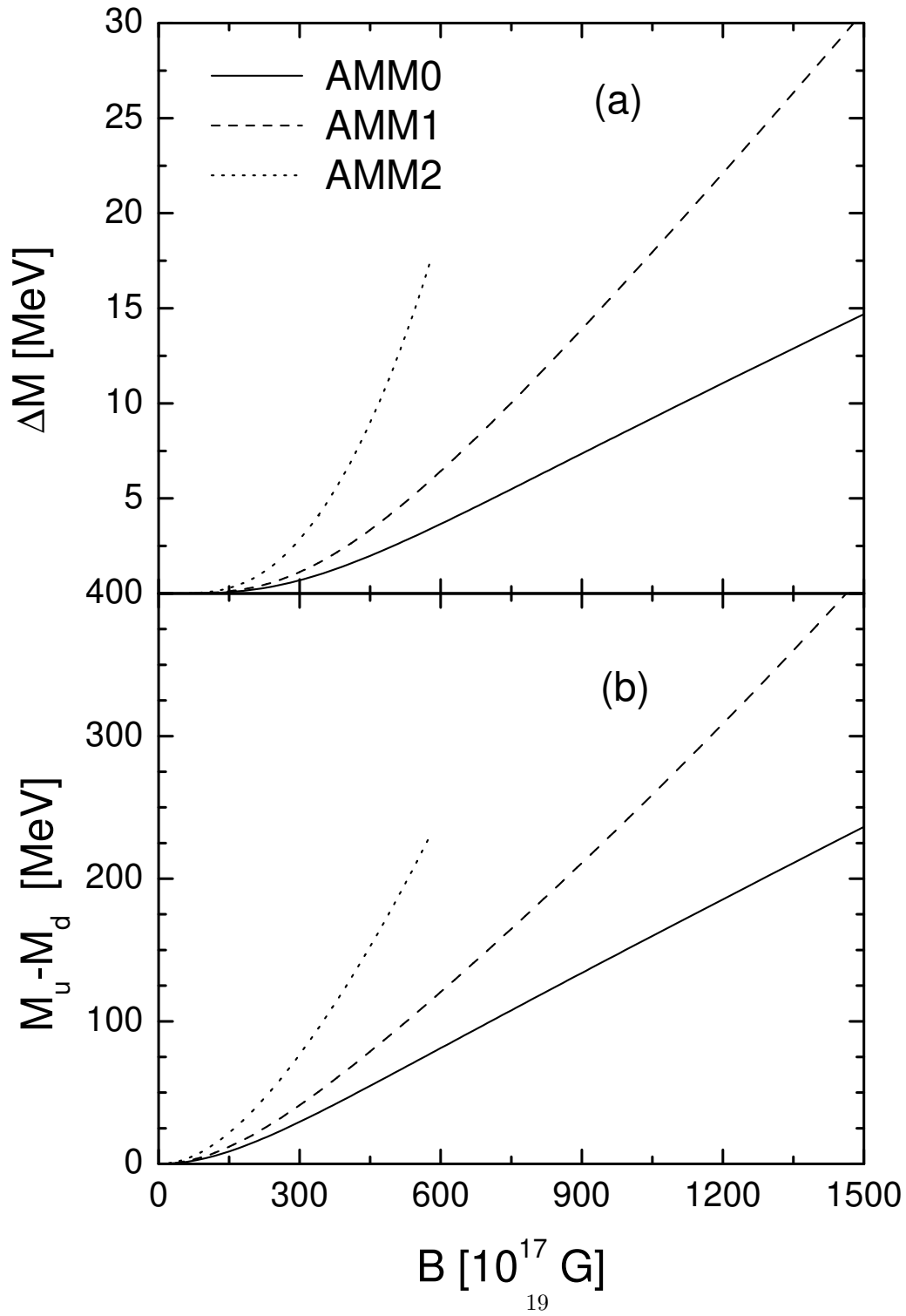


Figure 3: Two parameters characterizing the inputs used in the pion polarization function as functions of the magnetic intensity. In the upper panel (a) the deviation of the average  $(M_u + M_d)/2$  from the symmetrized  $M_{symm}$  values, in the lower panel the flavor splitting  $M_u - M_d$  are shown.

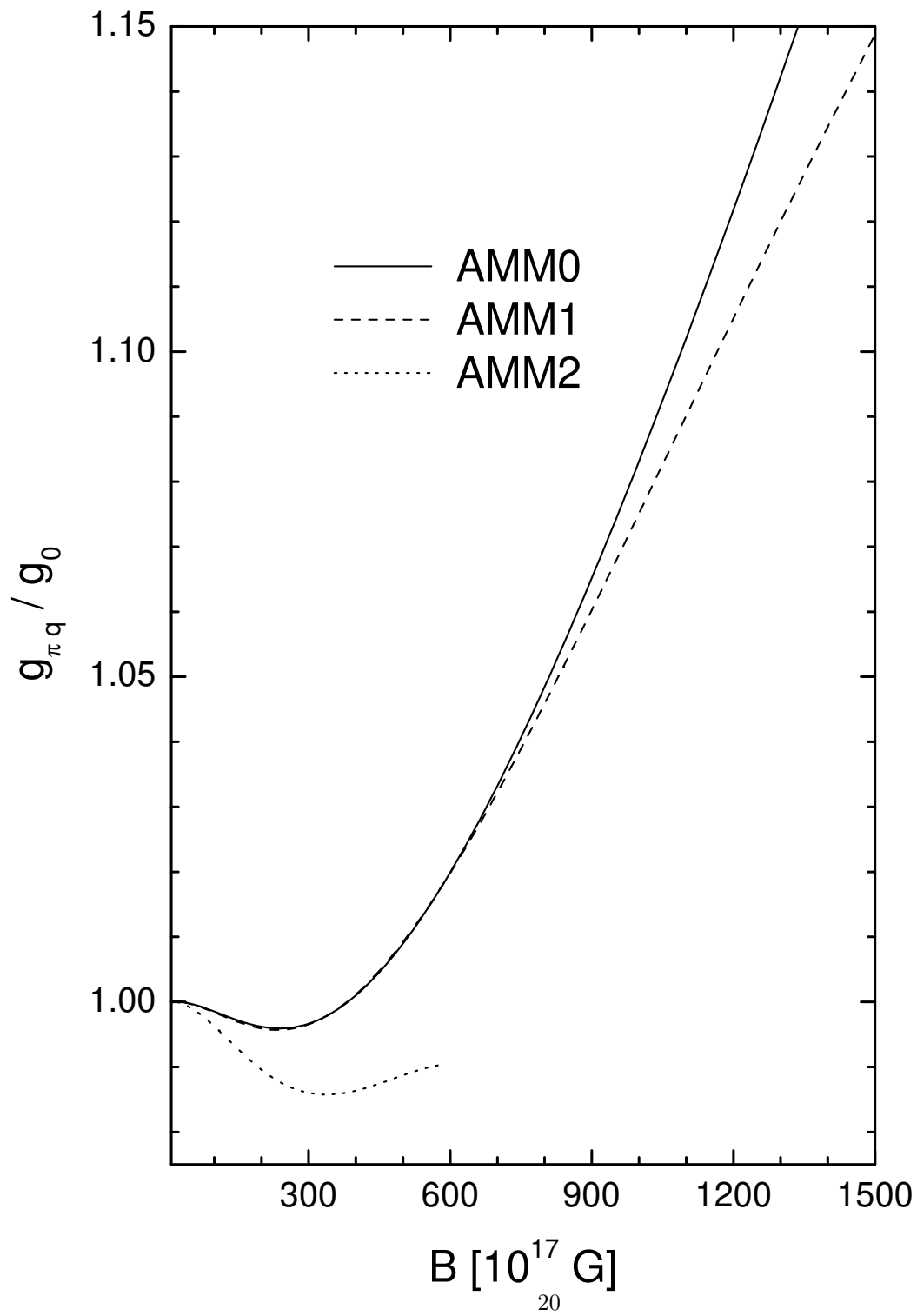


Figure 4: The pion-quark effective coupling as a function of the magnetic intensity evaluated using three different sets AMM0, AMM1 and AMM2.

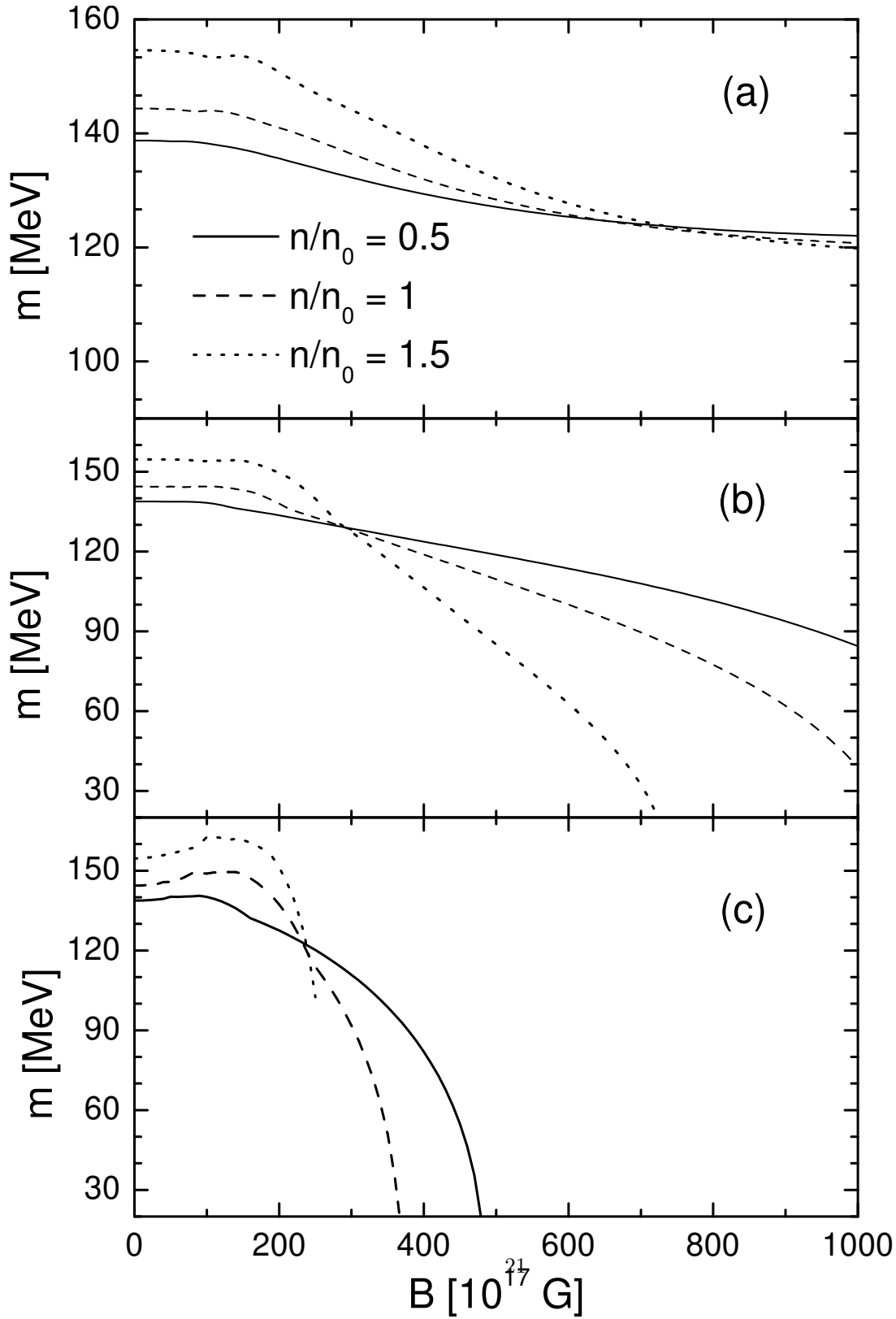


Figure 5: The effective pion mass as a function of the magnetic intensity for three different values of the baryon density using the sets AMM0 (a), AMM1 (b) and AMM2 (c). Isospin conservation under the condition of flavor symmetry  $n_u = n_d$  is considered.

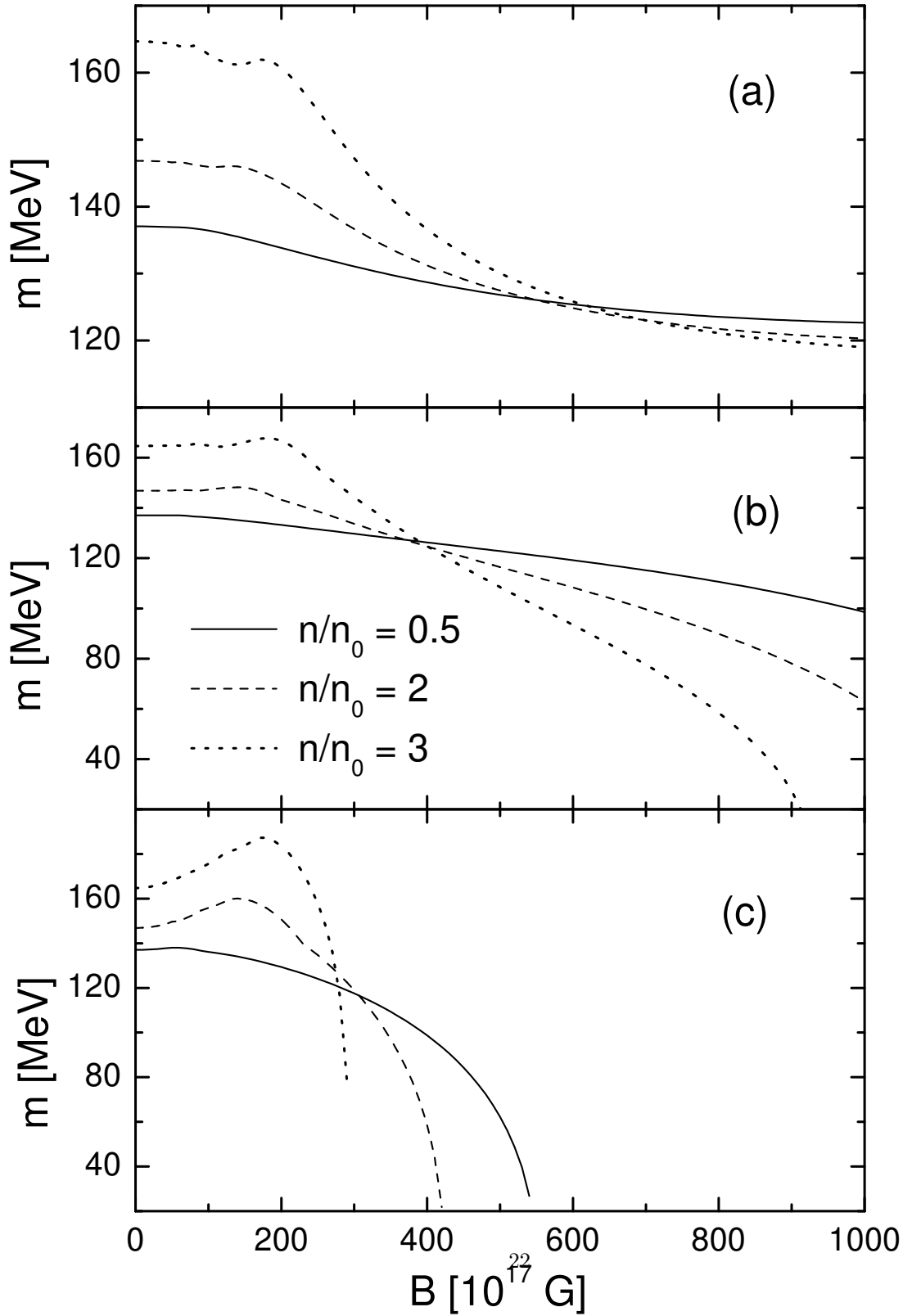


Figure 6: The effective pion mass as a function of the magnetic intensity for three different values of the baryon density using the sets AMM0 (a), AMM1 (b) and AMM2 (c). Isospin conservation under the condition of electrical neutrality  $2n_u = n_d$  is considered.

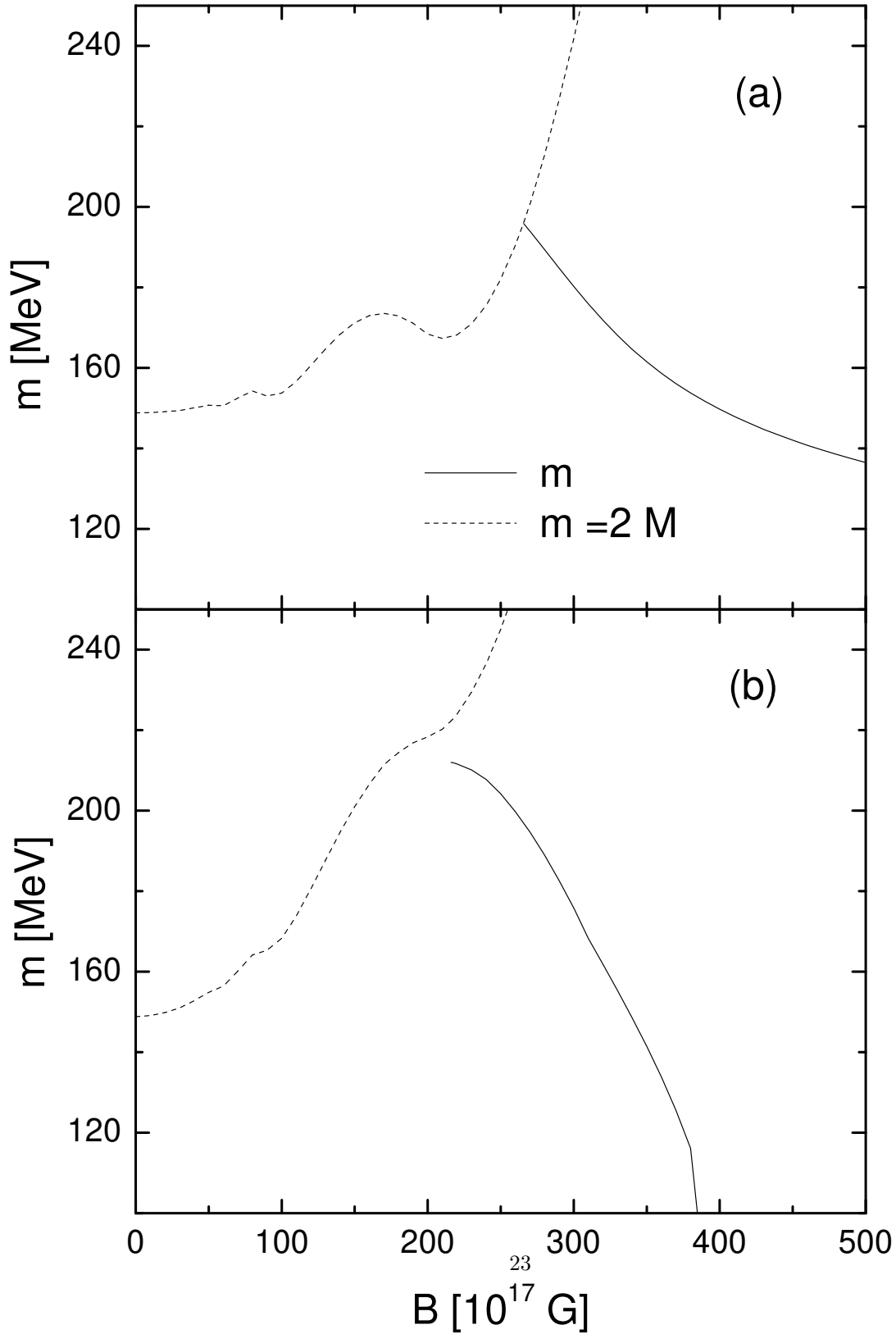


Figure 7: The threshold condition  $m = 2M$  for the stability of the solutions shown in the  $m - B$  plane, and the actual stable solutions of the pion mass for dense quark matter at  $n/n_0 = 4$  in the  $2n_u = n_d$  case. Different results corresponding to the AMM0 (a) or the AMM1 (b) sets are shown.

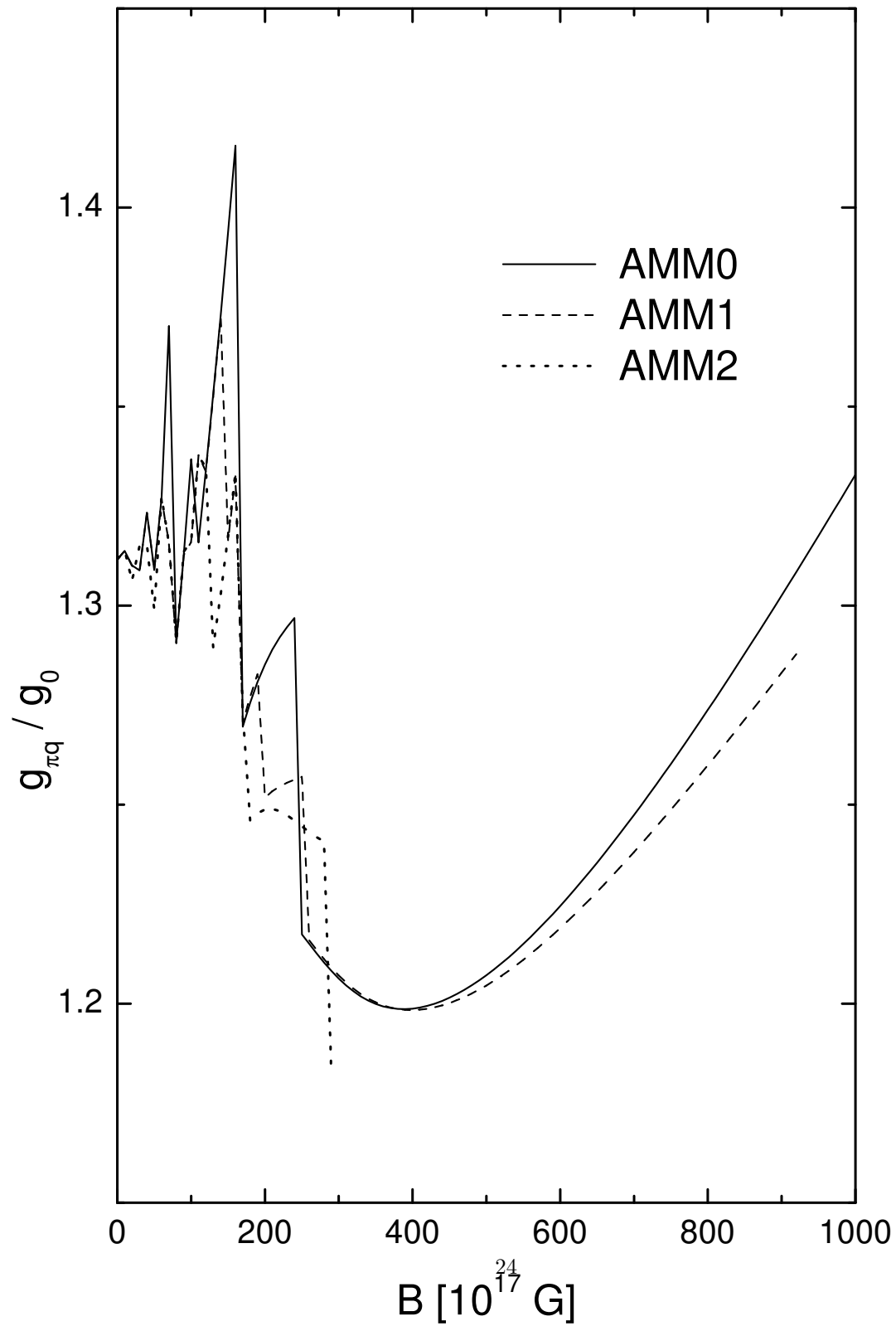


Figure 8: The pion-quark effective coupling as a function of the magnetic intensity evaluated in dense quark matter at  $n/n_0 = 3$  under the condition  $2n_u = n_d$ .